CALT-68-667
DoE RESEARCH AND
DEVELOPMENT REPORT
June 30, 1978
FERMILAB-PUB-78-170-E

Inclusive π^o and η Production in the All Neutral Mode from 100 GeV/c $\pi^- p$ Collisions

A. V. BARNES, G. C. FOX, R. G. KENNETT AND R. L. WALKER

California Institute of Technology, Pasadena, California 91125

and

O. I. DAHL, R. A. JOHNSON, R. W. KENNEY, A. OGAWA, AND M. PRIPSTEIN

Lawrence Berkeley Laboratory, Berkeley, California 94720

ABSTRACT

Results are given for π^o and η production in 100 GeV/c $\pi^- p$ collisions, summed over all final states with no charged particles present (the all neutral final states). The data are fitted for $x \gtrsim 0.6$ to a modification of triple Regge theory suggested by the multiperipheral model. We find good agreement between the values of the ρ and A_2 trajectories determined in the all neutral process, the full inclusive mode $\pi^- p \to (\pi^o, \eta)X$, and the exclusive reactions $\pi^- p \to (\pi^o, \eta)n$ The π^o production cross section shows evidence for a dip at $t \approx -0.5$ $(\mathrm{GeV/c})^2$ (the ρ wrong signature nonsense zero) whereas the η data are quite smooth in this region. These successful predictions for both the trajectory and residue function are striking evidence for the validity of triple Regge theory.

*Work supported in part by the Department of Energy under Contract No. EY76-C-03-0068 (Caltech) and Contract No. W-7405-Eng-48 (Lawrence Berkeley Laboratory).

I. Introduction

In this paper, we study experimentally the inclusive production of π^o's and η's from $\pi^- p$ collisions at 100 GeV/c in final states consisting of only neutral particles. We call this the NFS (neutral final state) mode hereafter. We show that an interesting generalization of Regge theory can be applied to these reactions and seems to be successful. This generalization is suggested by the multiperipheral model, as we show in Section II. Although this description is mainly a review of previous work, we present it in some detail because the generalization of triple Regge theory to the all neutral final state has not been discussed before. The essential result of this application is given by Eq. (9). In Section III we describe the apparatus and experimental definition of the NFS. In Section IV we compare our results to the generalized Regge theory developed in Section II.

II. Pseudo Regge Theory

In Fig. 1(a), we indicate the conventional multiperipheral model for the general multiparticle amplitude with n final particles[1]. Summing the squares of the amplitudes over multiplicities n, to find the total cross section, leads to the iterated ladder diagrams shown in Fig. 1(b). It is well known that the sum of these diagrams gives a total cross section with Regge behavior[1].

$$\sigma_{tot}\ (ab \to \text{anything}) \sim s^{\alpha-1} \tag{1}$$

as $s \to \infty$ where $\sqrt{s}$ is the center of mass energy of the incident particles a and b and α is the intercept of the exchanged Regge pole. Actually in a realistic model one finds not only more than one pole but also Regge cuts. In this qualitative review, we will not consider these complications and assume that (1) is valid with α as the intercept of the leading Regge trajectory.

Now it is easy to see that the mathematics that lead to Regge behavior from Fig. 1(b) must still be valid if we restrict the sum over intermediate particles i in the figure to any set of particles that obey some restrictive property P. Examples of possible properties for which some data exist, are:

(a) no restriction, i.e. the conventional total cross section (2a)

(b) all neutral particles; the NFS mode studied in this paper (2b)

(c) all mesons, e.g. the annihilation channels in $\bar{p}p$ collisions (2c)

(d) all nonstrange particles. (2d)

The restriction to particles obeying property P in Fig. 1(b) still leads to a Regge-like behavior because the ladder structure of the diagrams is preserved. It follows that one is then led to the prediction:

$$\sigma(ab \to \text{all particles obeying property P}) \approx s^{\tilde{\alpha}_P - 1} \tag{3}$$

which we call psuedo Regge theory. It is described for the all neutral case in Ref. 2.

In Eq. (3), the Regge intercepts, which we denote as $\tilde{\alpha}_P$, depend on the particular property P. For instance, one finds for the properties listed above in Eq. (2)

(a) $\tilde{\alpha}_P \approx 1$ for property (2a); it is the total cross section!

(b) $\tilde{\alpha}_P \approx -0.08$ for property (2b); see Fig. 5 and discussion in Section III.

(c) $\tilde{\alpha}_P \approx 0.5$ for property (2c); see Ref. 3 and Fig. 11 of Ref. 4.

(d) $\tilde{\alpha}_P \approx 1$ for property (2d) with a and b <u>nonstrange</u>, e.g. $\pi^{\pm}p$ collisions where the compilation of strange particle cross sections in Ref. 5 can be subtracted from the total cross section.

(d') $\tilde{\alpha}_P \approx 0.5$ for property (2d) with a and b <u>strange</u>, e.g. K^-K^+ collisions. This can be observed (with K^+ virtual) in $K^-p \to$ hyperon (Λ,Σ) plus nonstrange particles. The latter cross section is roughly equal to the difference between K^-p and K^+p total cross sections and so falls like (3) with $\tilde{\alpha}_P \sim 0.5$.

The pseudo Regge theory does not have as rich a structure as the ordinary theory. Although the pseudo trajectories can be formally defined as functions of t, we do not know any observable consequences except for the intercepts at t=0, where they can be seen through the restricted cross section predictions (3). In this paper, we will only consider the intercepts at t=0 and ignore the argument of $\tilde{\alpha}_P$. The pseudo theory not only predicts the energy dependence through (3) but also has nontrivial factorization predictions as the same pseudo pole will contribute to different reactions. For instance, one predicts the same energy dependence[6] for

$$\begin{aligned} &\pi^-p \to \text{all neutrals} \\ &K^-p \to \text{all neutrals} \\ \text{and} \quad &\bar{p}p \to \text{all neutrals}, \end{aligned} \tag{4}$$

which we study in a later paper using our data at 50, 100 and 200 GeV/c. The theory also predicts factorizable couplings whence, for instance, one can predict not only the energy dependence but also the relative magnitudes of K^-K^+, K^-p and $\bar{p}p$ to all neutrals. However, this is obviously hard to test. Note that one has to apply the factorization prediction with some care; for instance different pseudo poles contribute to the examples πp and $K^-K^+ \to$ nonstrange particles discussed above. This can be seen because the exchanged particles, e in Fig. 1, are completely different, being nonstrange in the πp and strange in the K^-K^+ case. There is thus no relation

between these reactions for the nonstrange final state even though one can predict the same energy dependence for the analogous full inclusive or all neutral final states (2a, 2b).

In this paper, we will consider an extension of pseudo Regge theory that corresponds to the triple Regge approach in the ordinary theory[7,8]. Take reactions of the form

$$\pi^- p \to (\pi^o, \eta) + \text{all neutrals} \tag{5a}$$

or more generally

$$ab \to c + \text{all particles obeying property P}, \tag{5b}$$

where particle c also obeys property P.

In Fig. 2, we contrast ordinary and pseudo triple Regge theory for these processes. The difference between (5a) and the conventional

$$\pi^- p \to (\pi^o, \eta) + \text{anything} \tag{6}$$

is just reflected in the difference between the cross section for the Reggeized ρ proton to either all neutrals (5a) or anything (6). This cross section has the behavior $(M^2)^{\tilde{\alpha}_P - 1}$ where $M^2 \approx s(1 - x)$ is missing mass squared in reactions (5a, 6). Here x is just the normal longitudinal (Feynman) momentum fraction of the final π^o or η in reactions (5a, 6). In either case, we find the differential cross section for the final observed particle π^o or η, to be

$$\frac{d^2\sigma}{dtdx} = f_P(t) \frac{(1 - x)^{\tilde{\alpha}_P(0) - 2\alpha_e(t)}}{s^{1-\tilde{\alpha}_P(0)}} , \tag{7}$$

where $f_P(t)$ is some function of t representing the product of ordinary and

triple Regge couplings, and t is the square of the momentum transfer between the incident π^- and the observed π^o or η. $\alpha_e(t)$ is the trajectory of the Regge pole exchanged between the incident π^- and the final π^o or η. This is the ρ for $\pi^- \to \pi^o$ and the A_2 for $\pi^- \to \eta$. Considering the full reaction (6), we substitute $\tilde{\alpha}_P(t) = \alpha_{\mathbb{P}}(0) = 1$, the Pomeron intercept, to give the conventional triple Regge formula;

$$\frac{d^2\sigma}{dtdx} = f_{FULL}(t)\ (1 - x)^{1-2\alpha_\rho(t)} \tag{8}$$

for $\pi^- p \to \pi^o X$, reaction (6), described by the dominant $\rho\rho$ Pomeron coupling.

To consider the reaction (5a), we need to know the correct value of $\tilde{\alpha}_P(0)$, which we will call $\tilde{\alpha}_{NFS}$. This is given, from (3), by the energy dependence of the all neutral total cross section, which is studied in Section III and Fig. 5, where we find

$$\tilde{\alpha}_{NFS} = -0.08 \pm 0.2. \tag{9a}$$

As discussed in Section III, the error is dominated by systematic problems in the definition of the all neutral final state. Thus we get our basic equation by substituting (9a) into (7) to find

$$\frac{d^2\sigma}{dtdx}\ (\text{for reaction (5a)}) = \frac{f_{NFS}(t)\ (1 - x)^{-0.08\ -\ 2\alpha_e(t)}}{s^{1.08}} \tag{9b}$$

We will use data at fixed s (corresponding to 100 GeV/c incident beam) and so we can test (9b) by fitting the x dependence of $\pi^- p \to \pi^o$ + all neutrals to a power of (1 - x) at fixed t. If the theory is correct, not only will this be a good fit but the powers of (1 - x) at different t will

enable one to extract $\alpha_e(t)$, the ρ and A_2 trajectories, and compare them to other determinations; namely those obtained from the s dependence of $\pi^- p \to (\pi^o,\eta)n$[9] and the x dependence of the full inclusive process, $\pi^- p \to (\pi^o,\eta)X$, using Eq. (8)[10]. In using (9b), we must remember the rather large error in $\tilde{\alpha}_{NFS}$. Note however this only gives an overall t independent shift to $\alpha_e(t)$ extracted from (9b).

Finally we shall continue along more theoretical lines and ask if a value of $\tilde{\alpha}_{NFS}$ near zero can be predicted. Again we will only give a qualitative discussion but believe that it contains the essential physics. In Fig. 1(c), we indicate a typical coupling to be used in our mulitperipheral model shown in Figs. 1 (a,b). We can exchange, among others, π and ρ mesons and possible intermediate particles are π^o, $\pi^o\pi^o$, η, K^o, etc. Now suppose we take the simplest model in which there is but one coupling, of size g_P, and an exchanged particle of intercept $\tilde{\alpha}_e$ where we set the slope $\alpha_e' = 0$. Then the value of the pseudo Regge intercept $\tilde{\alpha}_P$ is given by[1,2]

$$\tilde{\alpha}_P = 2\alpha_e - 1 + g_P^2 \quad . \tag{10}$$

In the NFS case $\alpha_e \sim 0.48$[9] correpsonding to the ρ and A_2 exchanged particles which would be expected to dominate. We can only reconcile this with the experimental observation $\alpha_{NFS} \sim -0.08$ if the coupling g_{NFS}^2 is small. Now we must ask if there is any type of simple multiperipheral model that could be consistent with nature? The only choice seems to be at present the so called multiperipheral cluster model where the intermediate "particles" i in Fig. 1(a) are low mass clusters of particles[4,11-13]. In this case, let us apply (10) first to the case when P has no restriction i.e. the total cross section. We find for the Pomeron intercept

$$\tilde{\alpha}_{FULL} = 1 = 2\alpha_e - 1 + g^2_{FULL} \tag{11}$$

or, for $\alpha_e = 0.48$, the well known result $g^2_{FULL} \approx 1$. Now we clearly get the all neutral final state when our clusters decay into only neutral particles. Thus

$$g^2_{NFS} = g^2_{FULL}\, P_{NFS},$$

or using (11)

$$\tilde{\alpha}_P \approx 2\alpha_e - 1 + P_{NFS} \tag{12}$$

where P_{NFS} is the probability that a cluster decays into neutral particles only. A small value of P_{NFS} would be expected; for instance there is strong evidence that the multiplicity of neutral particles is correlated positively with the charged multiplicity[11]. In other words, neutral particles do not like to be produced alone. Thus a value of $P_{NFS} \lesssim 0.1$, would be a reasonable estimate. Note on the other hand that if the intermediate particles were the three members of an isovector multiplet, e.g. $\pi^{o,\pm}$, then $P_{NFS} = 1/3$ and we predict a higher value for $\tilde{\alpha}_{NFS}$.

Note that (10) cannot be satisfied with our measurement $\tilde{\alpha}_{NFS} = -0.08$ and $\alpha_e = 0.48$, for any positive g^2_P. However the error in $\tilde{\alpha}_{NFS}$ and uncertainty in α_e would allow a positive $g^2_P \sim 0.05$. Further one might consider it more reasonable to use in (10) the value of α_e at $t \approx -0.1$ $(\mathrm{GeV}/c)^2$ ($p_\perp \sim 300$ MeV/c) i.e. $\alpha_e \sim 0.39$. With this choice, $\tilde{\alpha}_{NFS} = -0.08$ gives $g^2_P = 0.14$ from (10). However if one includes trajectories with non zero slopes in the multiperipheral model, one finds both pseudo poles and cuts in the output amplitude. One should also consider a multichannel problem with both π as well as ρ, A_2 as the exchanged particles. These complications will leave the critical Eq. (9b) qualitatively unchanged; one should sum over <u>all</u>

pseudo poles and cuts in the all neutral channel and not just use the effective intercept, (9a), obtained by fitting the all neutral cross section.

We emphasize that Eqs. (11) and (12) are only qualitative; however they serve to illustrate that the low value of $\tilde{\alpha}_{NFS}$ is a consequence of the small probability to find all neutral intermediate states in Fig. 1. The problems with the multiperipheral model are more severe with the large coupling full inclusive case (11) than the weak coupling NFS case (12). In fact the all neutral final state might prove to be an interesting reaction to investigate strong interaction dynamics in a weak coupling regime where it could well be cleaner than in the conventional full inclusive, large coupling, case. It is also worth noting that Eq. (3) may be more general than its multiperipheral deviation. The triple Regge generalization (9b) will follow in any theory that has (3) and the simple factorization associated with Regge poles. Other generalizations of (3) may be made using the technique introduced by Mueller[7]. For instance, Fig. 3(a) shows the pseudo Regge theory description of the process $\pi^- p \to \pi^o$ + all neutrals in the central region. This predicts, in the all neutral just as in the full inclusive case, a rapidity plateau where the π^o has small center of mass rapidity. As indicated in Fig. 3(b), the theory may also be applied to the two prong cross section in the same region[14], $\pi^- p \to 2$ charged particles + all neutrals. This figure illustrates that pseudo Regge theory can be applied to essentially any observable where one sums over reactions with any number of undetected neutrals. The success of the pseudo Regge theory in the triple Regge region shown by our data in Section IV, suggests that these other applications be explored further.

Finally we remark that taking the ratio of (8) and (9), we find that $(\pi^- p \to \pi^o + \text{all neutrals})/(\pi^- p \to \pi^o X)$ is a function of M^2 (namely $(M^2)^{\tilde{\alpha}(0)-1}$) times a function of t (namely $f_{NFS}(t)/f_{FULL}(t)$). Raja has postulated that such ratios be functions of M^2 only[15] and found evidence for this idea in $\bar{p}p$ interactions. In pseudo Regge theory, this is not generally true unless the ratio of couplings f_{NFS}/f_{FULL} is independent of t. This idea is only approximately correct as, for instance, our data shows that f_{NFS} has more structure at $t \sim -0.5$ $(GeV/c)^2$ than f_{FULL}. Inclusion of other terms in (8) and (9) (e.g. the $\rho\rho f$ triple Regge term in (8)) will also render Raja's hypothesis invalid.

III. The Neutral Final State Experiment

The experimental apparatus is shown in Fig. 4. The essential feature is the photon detector which has already been used in several previous experiments. These were $\pi^- p \to \pi^o n$[9] (Fermilab Experiment 111) and inclusive π^o production at large transverse momentum[16] (Fermilab Experiment 268). The experiment described in this paper was Fermilab Experiment 350 and, like its predecessors, it was performed in the M2 beam line of the meson laboratory. The photon detector is described briefly in Ref. 9. It has good position and energy resolution; for 100 GeV photons these are .5 mm and 2 GeV respectively. A significant effort was made to improve the energy resolution for E350 as measurement of the shape of the energy distribution is a major goal of this experiment. The techniques used are described in Ref. 10.

The all neutral final state was recognized by the scintillation counters $A_{0\to4}$ shown in Fig. 4. Events with no signal in these counters were tagged as the all neutral final state. There was no problem in separating these from the charged multiplicity two (or greater) final states. The response of the counters to the latter was determined from the interactions of positively charged beam particles in the target and from cosmic rays.

We are interested in two types of measurement. The simplest is just the total all neutral cross section which will be described in this section. In Section IV we will describe the inclusive measurements, $\pi^- p \to \pi^o$ or η plus all neutrals. Cherenkov counters in the beam enable one to select π^-, K^- and $\bar{p}$ components with good reliability; however in this paper we will only discuss data with negative pions.

Measurement of the all neutral cross section is simple in principle. One needs only to know the number of events that satisfy the NFS requirement for a given incident beam flux. One must also subtract the target empty contribution but this is small, being 4% of the target full rate. This gives a raw cross section at 100 GeV,

$$\sigma_{raw}(\pi^- p \to \text{all neutrals}) = 23\ \mu b.$$

However one must make various corrections, which are detailed in Table 1, and end up with a final cross section,

$$\sigma_{corrected}(\pi^- p \to \text{all neutrals}) = 40 \pm 6\ \mu b. \qquad (13)$$

which is compared with other measurements in Fig. 5. The large error in (13) comes entirely from the systematic errors listed in Table 1. The statistical error from our half a million NFS events is obviously negligible! This large number of triggers was not of course to determine the total cross section but the π^o inclusive data discussed in the next section.

We fail to trigger on NFS events for four main reasons:

(a) Conversion of photons from π^o and η in the target will make the event look as though a charged particle was present. Dalitz decay of the π^o and charged particle decays of η's have the same effect. We have a 10% chance of vetoing a π^o and a 40% chance for an η. The first entry in Table

1 comes from guessing that there are 2 ± 1 π^o's in each event and ignoring η's. The corresponding π^o multiplicity and limit on η production in ordinary events may be found in Refs. 4 and 20 respectively.

(b) Strange particles that decay into charged particles, $\Lambda \to p\pi^-$ or $K^o \to \pi^+\pi^-$, before they reach the scintillation counters $A_{0\to4}$ will be vetoed. This correction depends on both the number and energy spectrum of the particles. It is difficult to make a reliable estimate, We guessed that the main correction is due to slow Λ's occuring in 15% of the events.

(c) In the remaining ($\sim$ 85%) of the events baryon number is conserved by the production of neutrons. There is a small probability for these to interact in the scintillation counters and veto the event. This correction has already been studied and is shown in the third line of Table 3[21].

(d) Finally delta rays produced by the incident beam will veto the event but again this correction was studied for the $\pi^-p \to \pi^o n$ and ηn experiment[21]. It is shown in the fourth line of Table 1.

The last two entries in Table 1 are quite conventional and need no comment.

The reader will have realized that this is not the perfect experiment for measuring the all neutral final state. We just used a simple method that could record the neutral final state parasitically during the main task of the experiment - measurement of the full inclusive π^o and η cross section[10]. We consider our apparatus appropriate for the first inclusive π^o NFS experiment. However the new results on this process in Section IV are extremely interesting and warrant a more careful investigation with a less biased NFS trigger.

We now return to Fig. 5 which shows a fit to Eq. (3) with $\tilde{\alpha}_{NFS} = -0.08$. We emphasize that the biases a) → c) are present to some degree in all the other experiments in Fig. 5. It is not clear how the corresponding corrections have been made in most of the other experiments and so the exact value of $\tilde{\alpha}_{NFS}$ cannot be taken very seriously; we estimate that error in the -0.08 value for $\tilde{\alpha}_{NFS}$ could be at least 0.2.

IV. π^o and η Inclusive NFS Measurements

We now turn to reaction (5a), $\pi^- p \to (\pi^o, \eta)$ + all neutrals. The π^o and η were detected through their two photon decay in the photon detector shown in Fig. 4. In the corresponding full inclusive experiment[10], we only triggered on events in which the energy in the photon detector was above a certain threshold. This was not necessary for the NFS data. We recorded on tape all events that satisfied the NFS requirement from the scintillation counters, $A_{0\to4}$, without any requirement at all on the photon detector. This gives us reasonable acceptance for Feynman $x \geq 0.1$ in the c.m.s. However we will only discuss data with $x \gtrsim 0.6$, the region covered by the full inclusive experiment[10]. The data were analyzed in an identical way to Ref. 10; there was a slightly higher background of uncorrelated two photon pairs under the π^o and η mass peaks which is detailed in Table 2. For π^o triggers, 80% of the events have only two photons in the detector with a 0.1% background under the π^o peak. The remaining 20% of the events have more than two photons in the detector with a much higher background of 18% under the π^o peak. The backgrounds decrease strongly with increasing energy but have little $p_\perp$ dependence. The η data have substantially higher background as shown in Table 2. All data presented here have had the background subtracted, as described in Ref. 10, by using mass regions outside the peaks.

The data are shown in Figs. 6-8. The last two corrections in Table 1 have been applied but not the first four. Let us first discuss the energy spectra shown in Figs. 6 and 7. Here x has been defined as the ratio of $\pi^o(\eta)$ laboratory energy to the maximum possible energy for the given t value (i.e. the value for $\pi^- p \to (\pi^o,\eta)n$ at the same t value). We can only show a selection of data for representative t values in the region $0 \lesssim -t \lesssim 3\ (\mathrm{GeV/c})^2$ covered by our experiment. We immediately notice in Figs. 6 and 7 the very striking change in shape of the energy spectra with t; at low t we have a peak at $x \sim 1$ while at higher t the cross section is concentrated at low x. This is beautifully explained in pseudo triple Regge theory, Eq. (9), by the change of $\alpha_e(t)$ with t. Just as in the full inclusive case, the π^o and η production reactions are particularly nice because they allow only one dominant exchanged trajectory - the ρ and A_2 for π^o and η respectively. In Fig. 9(a) and (d) we show the ρ and A_2 trajectories extracted from the data exemplified in Figs. 6 and 7. Here we fit the data with $0.57 < x < 0.98$ to the sum of a pseudo triple Regge term (7) and a low mass resonance contribution. The latter is dominated by $\pi^- p \to \pi^o n$ and is clearly evident for the lower t values. One can also estimate the cross section $\pi^- p \to \pi^o(\Delta^o_{1232} \to n\pi^o)$ as roughly one third that of $\pi^- p \to \pi^o n$. At low -t the low mass peak is consistent in normalization with just these two terms. At $t \sim -0.4\ (\mathrm{GeV/c})^2$, the observed peak is 40% bigger than our expectation from n and Δ^o alone. Presumably other low mass resonances with flatter t dependence are contributing. In any case, by $t \sim -0.6\ (\mathrm{GeV/c})^2$, this low mass resonance term has a negligible effect. We do not fit in the region where this non-Regge term is important but include it so that we can correctly get the spill down from high x to low x due to our finite resolution. Actually the sharp drop $x \gtrsim 1$ in the low -t

NFS data is the best measure of our energy resolution. Detailed fits to this region give an energy resolution $\sigma_E = 1.6\%$ at 100 GeV/c. As explained in Ref. 10, we do not have any other good way of finding our resolution because it is dominated, not by electromagnetic shower statistics, but by our imperfect knowledge of the (time dependence of the) gains of our phototubes.

To return to the physics, we remark that the ρ and A_2 trajectories shown in Fig. 9 are in good but not perfect agreement with those from $\pi^- p \to (\pi^o, \eta)n$. There is a tendency in π^o production for the trajectory extracted from the NFS data to be a little below the $\pi^- p \to \pi^o n$ value. Fitting over a smaller x range, $0.76 < x < 0.98$, raises the extracted trajectory by ≈ 0.1 for $-t > 0.4$ $(\text{GeV/c})^2$, giving better agreement with the $\pi^- p \to \pi^o n$ determination. (See Fig. 9(b).) Note that the expansion parameter in (pseudo) triple Regge theory is, for small t, s/M^2 (where M^2 is the missing mass) or $1/(1 - x)$. This is certainly not large for $x \sim 0.6$ and there is no a priori reason why the theory should work so well down to small x values. Further we must remember that, as discussed in Section III, this is not a perfect experiment. Our NFS definition is biased and this bias depends both on the π^o multiplicity and the strange particle content of the final state. One would expect this bias to depend on M^2 and hence on x. Thus (small) shifts in α are to be expected from the corrections due to the biased NFS definition. One must also remember that the error in the determination of $\tilde{\alpha}_{NFS}$ causes a t independent shift in $\alpha_e(t)$ as discussed in Section II. However we think that the simple theory gives an impressive fit to the data. There seems little doubt that pseudo triple Regge theory is basically correct and describes the bulk of the NFS data. It describes the NFS data as well as ordinary triple Regge theory describes the full inclusive cross section. In fact, pseudo Regge theory seems to work down to lower x than the ordinary theory. In the

latter case the theoretical fits, in Ref. 10, lie below the data for $x \leq 0.7$. We can understand this by supposing that there are both triple Regge (leading) and central region ($x \sim 0$) terms. The tail of the latter extends to high x and causes the full inclusive discrepancy; in the NFS case one would expect a smaller central region term as its size is governed by the parameter g_P^2 which is much smaller in NFS compared to full inclusive case. In Fig. 9 (c) we compare $\alpha_\rho(t)$ from the all neutral and full inclusive final states. Notice these similar trajectories were determined from very different energy spectra; from Eq. (7), the NFS case is sharper as x goes to 1, by a factor $1/(1 - x)^{1.08}$. After showing the conventional fall with t for $-t \lesssim 1.5$ $(\mathrm{GeV}/c)^2$, <u>both</u> trajectories level off at a value of around -0.6 with little or no t dependence. As we discussed in Ref. 10, the constituent interchange model predicts such a behavior with the asymptotic level being -1[22]. We seem to find a significantly higher value (a fit with α fixed at -1 is shown for the highest -t bin of Fig. 6) but this may be a transition region in t; the trajectory could well go lower at higher -t values.

Finally in Fig. 8, we show the t dependence of the cross section for various x bins. There is a sharp peak at low t with a break or dip at $t \sim -0.5$ $(\mathrm{GeV}/c)^2$. The latter is shown more clearly in Fig. 10(a) where we plot the pseudo triple Regge residue function G(t) defined by

$$\frac{d^2\sigma}{dtdx} = G(t)(1 - x)^{-0.08 - 2\alpha_e(t)} \tag{14}$$

There is a clear dip at $t = -0.5$ $(\mathrm{GeV}/c)^2$ which it is natural to associate with the wrong signature nonsense zero of the ρ. There is no structure in the A_2 exchange residue at this point. We believe that the observation of this dip is very significant. Up to now it has only been seen in $\pi^- p \to \pi^0 n$

and related amplitudes. The folklore associates the dip with the spinflip nature of the $\pi^- p \to \pi^o n$ cross section[23]. The NFS zero is clearly seen in Fig. 8 for $0.71 \leq x \leq 0.91$ where the missing mass M^2 is large and there is no reason to think there is any simple spin structure. In the full inclusive case, Ref. 10, we also found a dip in the residue function but it was only present when we fitted for large x and was not visible in the t dependent cross sections analogous to Fig. 8. Simple Regge theory seems to work over a larger range of x for the NFS compared to full inclusive x. We have shown this for both the trajectory and the residue function. It is attractive to associate this with the weak coupling nature of the NFS.

In Fig. 10(b) we compare the ratio of π and η production for the NFS and full inclusive cases. The NFS value is systematically larger but we do not know if this is significant. Returning to Fig. 8, we have sketched in the t dependence of the full inclusive data at high -t; we see that both the NFS and full inclusive cross sections fall with roughly the same t dependence in the region ($-t \gtrsim 1.5$ $(\mathrm{GeV}/c)^2$) where the trajectory values have levelled off.

In conclusion we would like to emphasize the agreement of the all neutral data with the simple ideas of pseudo triple Regge theory. This theory was motivated by the multiperipheral model but could well be more general. The very similar behavior exhibited by the NFS and full inclusive cross sections and the success of naïve Regge theory should be valuable constraints on theories of the strong interactions. In particular the dip seen for ρ and not A_2 exchange at $t \sim -0.5$ $(\mathrm{GeV}/c)^2$ is significant support for the simple Regge theory (wrong signature nonsense zero) explanation of such dips in two body processes.

Acknowledgements

We would like to thank Joel Mellema and Alvin Tollestrup for their invaluable help at the start of this experiment. Bruce Cortez, David Hermeyer and Aileen Stone were very helpful in the analysis and running of the experiment. Rosemary Kennett would like to thank the Fannie and John Hertz Foundation for Fellowship support.

Table 1

Efficiency for Detecting All Neutral Final State

	Value	Absolute Error
Photon conversion and π^o Dalitz pair decay	.81	.10
Strange particle veto	.90	.05
Neutron veto	.98	.01
Delta rays	.90	.04
Beam attenuation in target	.97	.00
Cherenkov counter efficiency	.92	.03
Total	.57	.08

Table 2

Backgrounds Under the π^o and η Peak ($x > 0.57$)

Produced Particle	Photons in Detector	Fraction of Events	Background/Signal
π^o	2	0.8	.001
π^o	>2*	0.2	.18
η	2	0.9	.07
η	>2*	0.1	10

*π^o's have more mulitphoton events than η's because of the large 2 π^o cross section.

References

1. D. Horn and F. Zachariasen, Hadron Physics at Very High Energies, W. A. Benjamin (1973).
2. P. W. Coulter and D. R. Snider, Phys. Rev. D8, 4055 (1973).
3. P. D. Ting, Phys. Rev. 181, 1942 (1969). Note that the $\bar{p}p$ annihilation cross section is roughly equal to the difference between the $\bar{p}p$ and pp total cross sections.
4. J. Whitmore, Phys. Reports 27C, 187 (1976).
5. E. Bracci et al., Compilation of Cross Sections I - π^- and π^+ Induced Reactions, CERN/HERA 72-1 (unpublished) (1972).
6. R. E. Ansorge et al., Phys. Letters 59B, 299 (1975). This has a compilation of $\bar{p}p \to$ all neutrals data.
7. A. H. Mueller, Phys. Rev. D2, 2963 (1970); Phys. Rev. D4, 150 (1971).
8. R. D. Field and G. C. Fox, Nucl. Phys. B80, 367 (1974).
9. A. V. Barnes et al., Phys. Rev. Letters 37, 76 (1976); O. I. Dahl et al., Phys. Rev. Letters 37, 80 (1976).
10. A. V. Barnes et al., "Inclusive π^o and η Production from 100 GeV/c $\pi^{\pm}p$ Collisions in the triple Regge Region," CALT-68-664, preprint (1978).
11. A. W. Chao and C. Quigg, Phys. Rev. D9, 2016 (1974).
12. L. Foa, Phys. Reports 22C, 1 (1975).
13. K. Eggert et al., Nucl. Phys. B86, 201 (1975).
14. G. A. Koelsch and D. R. Snider, Phys. Rev. D14, 1889 (1976).
15. R. Raja, "Observation of a New Regularity in Hadronic Spectra," Fermilab preprint (1977).
16. G. Donaldson et al., Phys. Rev. Letters 36, 1110 (1976) and Phys. Letters 73B, 375 (1978).
17. V. Polychronakos et al., Phys. Rev. D11, 2400 (1975).
18. W. D. Apel et al., Phys. Letters B46, 459 (1973).

19. H. R. Crouch Jr. et al., Phys. Rev. Letters 21, 845 (1968).

20. K. J. Anderson et al., Phys. Rev. Letters 37, 799 (1976).

21. R. A. Johnson, thesis, Lawrence Berkeley Laboratory Report No. LBL-4610, 1975 (unpublished).

22. D. Sivers, S. Brodsky and R. Blankenbecler, Phys. Reports 23C, 1 (1976).

23. A. Irving and R. P. Worden, Phys. Reports 34, 117 (1977).

Figure Captions

Figure 1: The multiperipheral model for (a) the amplitude for $ab \to n$ particles and (b) the total cross section. In (c) we show the basic coupling appearing in the ladders of 1(b).

Figure 2: Comparison of triple Regge theory for $\pi^- p \to \pi^o$ plus either any other particles (the full inclusive) or any other neutral particles (the NFS inclusive mode).

Figure 3: (a) A Mueller diagram[7)] contributing to $\pi^- p \to \pi^o$ + all neutrals for π^o's in the central region.

(b) A Mueller diagram contributing to $\pi^- p \to h^+ h^-$ + all neutrals for two charged hadrons $h^+ h^-$ in the central region.

Figure 4: The experimental apparatus discussed in Section III and Refs. 9 and 10.

Figure 5: A compilation of data on $\pi^- p$ to all neutrals from Refs. 4, 5 and 17 - 19. Also shown is the point at 100 GeV/c from this experiment. The line corresponding to Eq. (3) is plotted with $\tilde{\alpha}_{NFS} = -0.08$.

Figure 6: Data on $\pi^- p \to \pi^o$ plus all neutrals as a function of x for selected t bins. The fitted curves are described in the text and the values of α (the ρ trajectory according to pseudo triple Regge theory) are plotted for all t bins in Fig. 9(a).

Figure 7: Data on $\pi^- p \to \eta$ plus all neutrals as a function of x for selected t bins. The fitted curves are described in the text and the values of α (the A_2 trajectory according to pseudo triple Regge theory) are plotted for all t bins in Fig. 9(d).

Figure 8: The t dependence of the $\pi^- p \to \pi^o$ plus all neutrals cross section for bins in x. We also show a paramterization of the $\pi^- p \to \pi^o n$ data from Ref. 9. The lines drawn through the large t data points have the same slope for all x bins. This slope was determined from a fit to the full inclusive data ($\pi^- p \to \pi^o$ plus anything) in Ref. 10.

Figure 9: The t dependence of $\alpha_e(t)$ determined from fits using (7) and illustrated in Figs. 6 and 7. A linear trajectory passing through the ρ, A_2 and g masses is shown in Figs. 9(a) and (d). In detail we have:

(a) $\alpha_\rho(t)$ from $\pi^- p \to \pi^o$ plus all neutrals. Fits are illustrated in Fig. 6 and were performed over the region $0.57 \leq x \leq 0.98$.

(b) Difference between $\alpha_\rho(t)$ determined as in (a) and that from smaller x range, $0.76 \leq x \leq 0.98$.

(c) Comparison of $\alpha_\rho(t)$ shown in Fig. 9(a) and that from Triple Regge theory for the full inclusive data. The latter comes from the fits in Ref. 10 for $x > 0.81$.

(d) $\alpha_{A_2}(t)$ from $\pi^- p \to \eta$ plus all neutrals. Fits are illustrated in Fig. 7 and were performed over region $0.57 \leq x \leq 0.98$.

Figure 10: (a) The residue functions G(t) defined in (14) for ρ and A_2 Regge poles in the all neutral final state. The dip in the ρ case at $t \sim -0.5\ (\mathrm{GeV/c})^2$ is quite apparent.

(b) The ratio of η to π production (integrated over $x \geq 0.7$) as a function of t in the all neutral final state is compared with the full inclusive results of Ref. 10.

(a) Multiperipheral Model for ab → n Particles

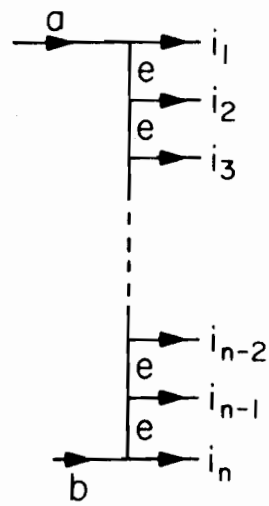

a, b Incident Particles
e Exchanged Particles
i Intermediate State Particles

(b) Multiperipheral Model for Total Cross Section

σ (ab → all particles obeying property P) ~ $\sum_n$ Intermediate Particles i Obey Property P

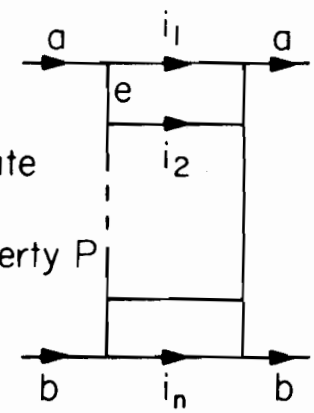

~

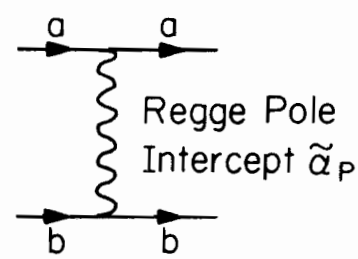

(c) A Multiperipheral Coupling

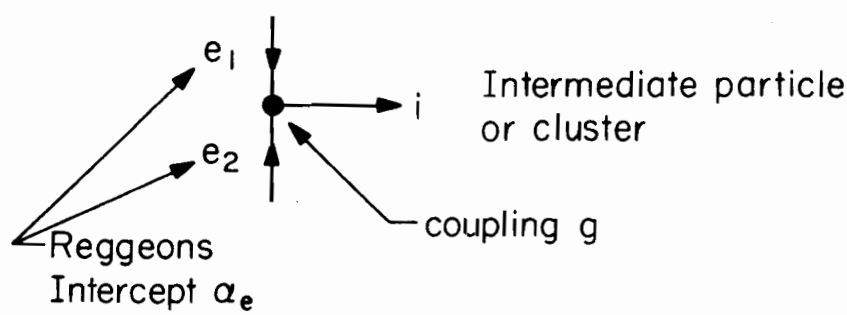

Fig. 1

Triple Regge Formalism

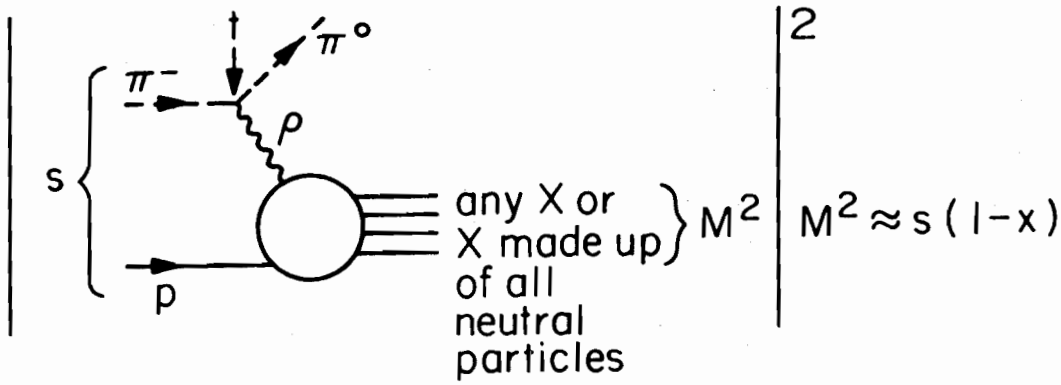

=

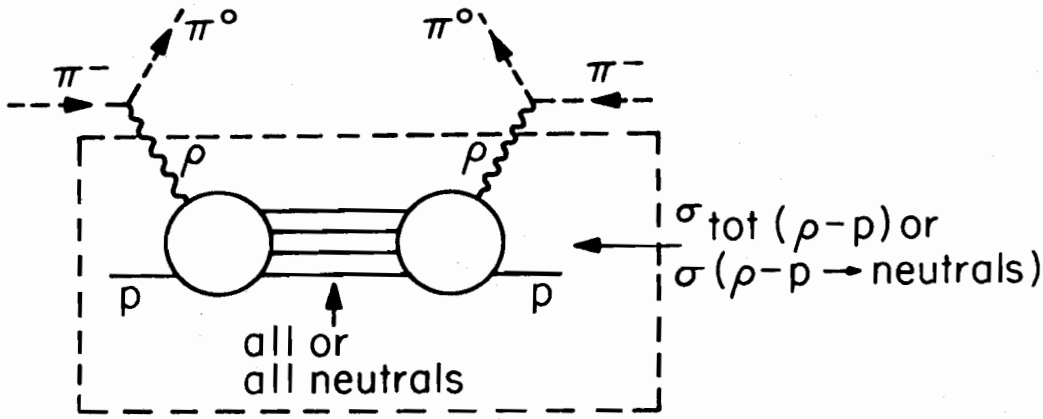

=

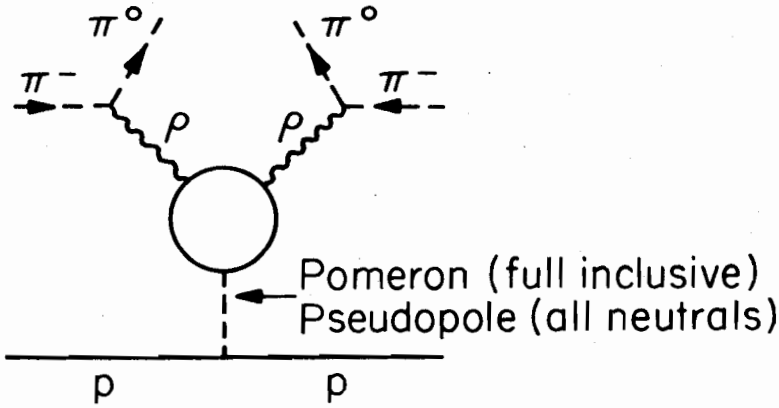

Fig. 2

(a) $\pi^- p \rightarrow \pi^\circ$ plus all Neutrals

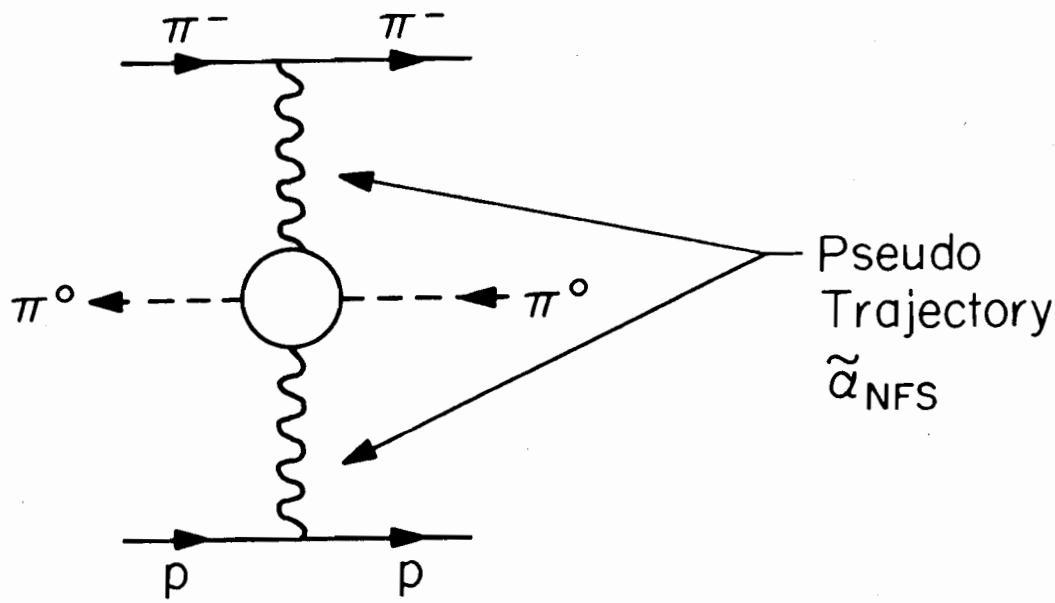

(b) $\pi^- p \rightarrow h^+ h^-$ plus all Neutrals ($\pi^- p \rightarrow$ 2 prongs)

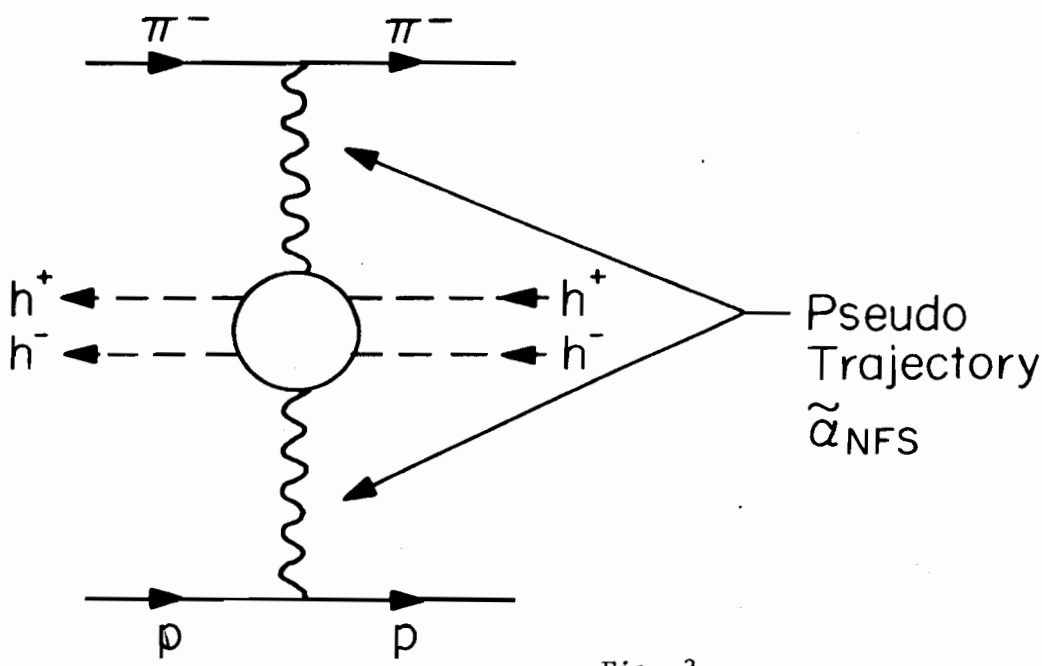

Fig. 3

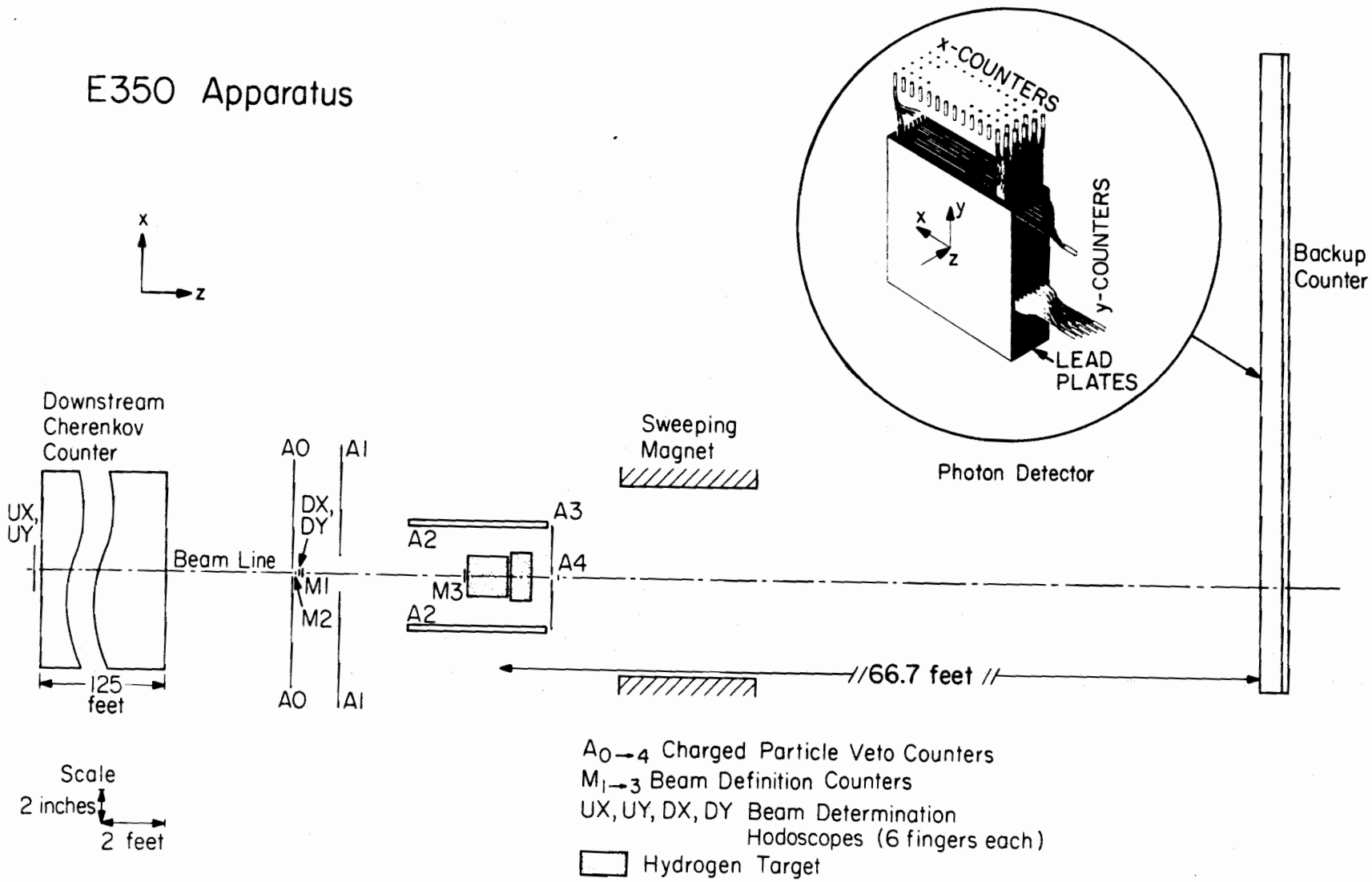
E350 Apparatus
x
z
Downstream
Cherenkov
Counter
UX,
UY
Beam Line
A0
A1
DX,
DY
M1
M2
A0
A1
A2
A3
A4
M3
A2
Sweeping
Magnet
x-COUNTERS
y-COUNTERS
LEAD
PLATES
Photon Detector
Backup
Counter
125
feet
66.7 feet
Scale
2 inches
2 feet
A0→4 Charged Particle Veto Counters
M1→3 Beam Definition Counters
UX, UY, DX, DY Beam Determination
Hodoscopes (6 fingers each)
Hydrogen Target

Fig. 4

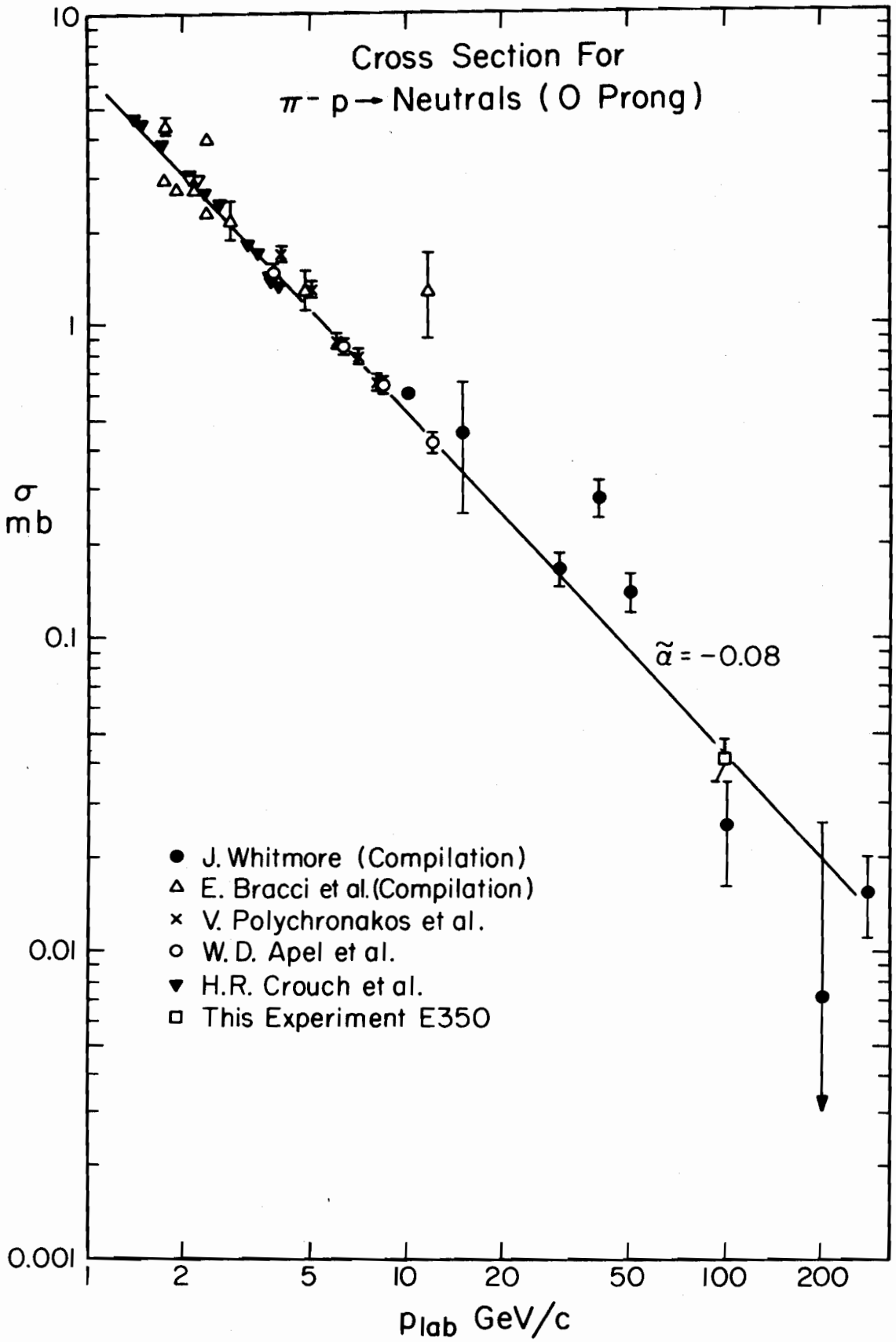
Cross Section For
$\pi^- p \rightarrow$ Neutrals (O Prong)
σ mb
p_{lab} GeV/c
$\tilde{\alpha} = -0.08$
J. Whitmore (Compilation)
E. Bracci et al.(Compilation)
V. Polychronakos et al.
W. D. Apel et al.
H.R. Crouch et al.
This Experiment E350
10
1
0.1
0.01
0.001
1
2
5
10
20
50
100
200

Fig. 5

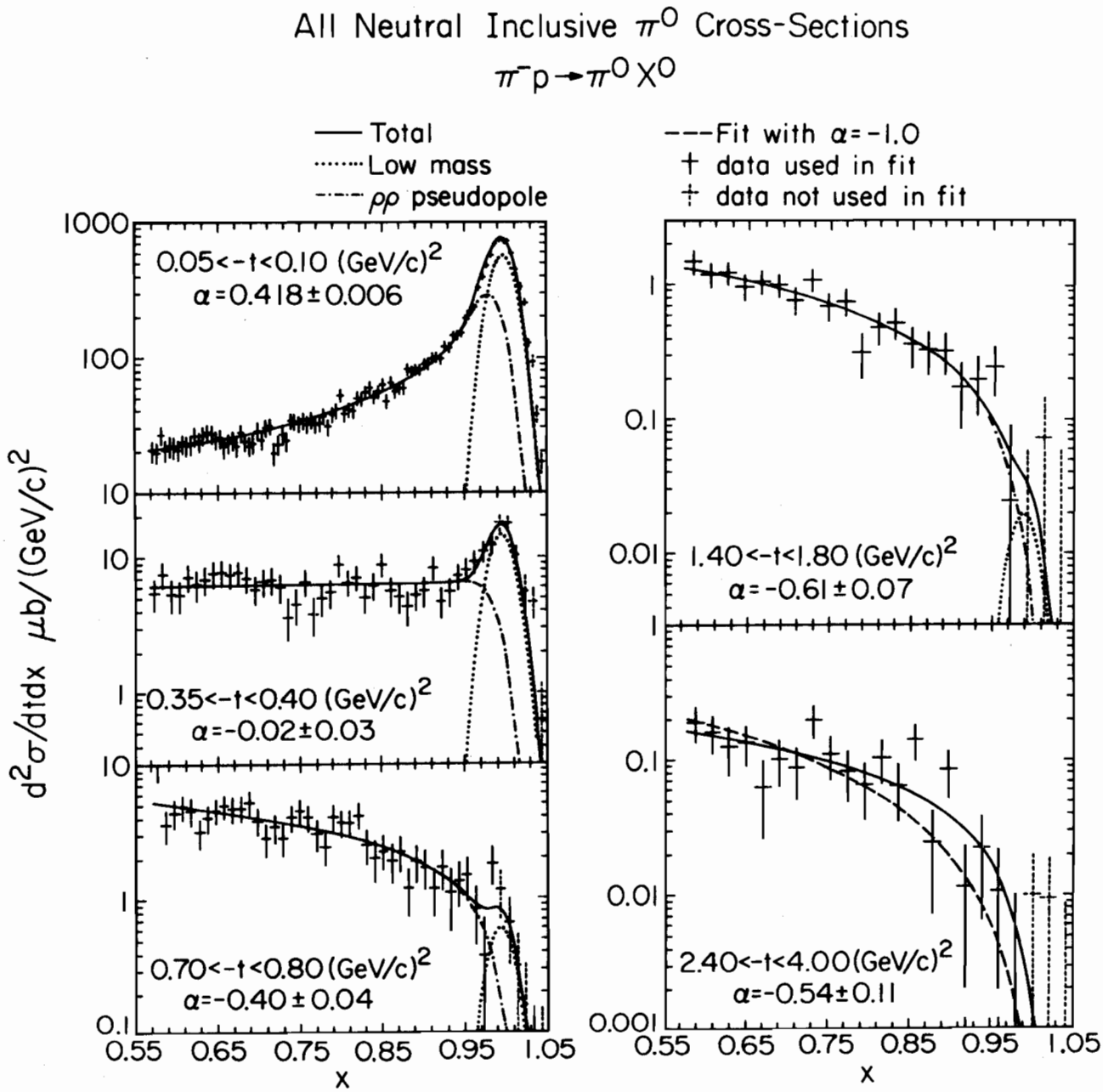
All Neutral Inclusive π^0 Cross-Sections
$\pi^- p \rightarrow \pi^0 X^0$
Total
Low mass
$\rho\rho$ pseudopole
Fit with $\alpha = -1.0$
data used in fit
data not used in fit
$0.05 < -t < 0.10$ (GeV/c)^2
$\alpha = 0.418 \pm 0.006$
$0.35 < -t < 0.40$ (GeV/c)^2
$\alpha = -0.02 \pm 0.03$
$0.70 < -t < 0.80$ (GeV/c)^2
$\alpha = -0.40 \pm 0.04$
$1.40 < -t < 1.80$ (GeV/c)^2
$\alpha = -0.61 \pm 0.07$
$2.40 < -t < 4.00$ (GeV/c)^2
$\alpha = -0.54 \pm 0.11$
$d^2\sigma/dtdx$ μb/(GeV/c)^2
x

Fig. 6

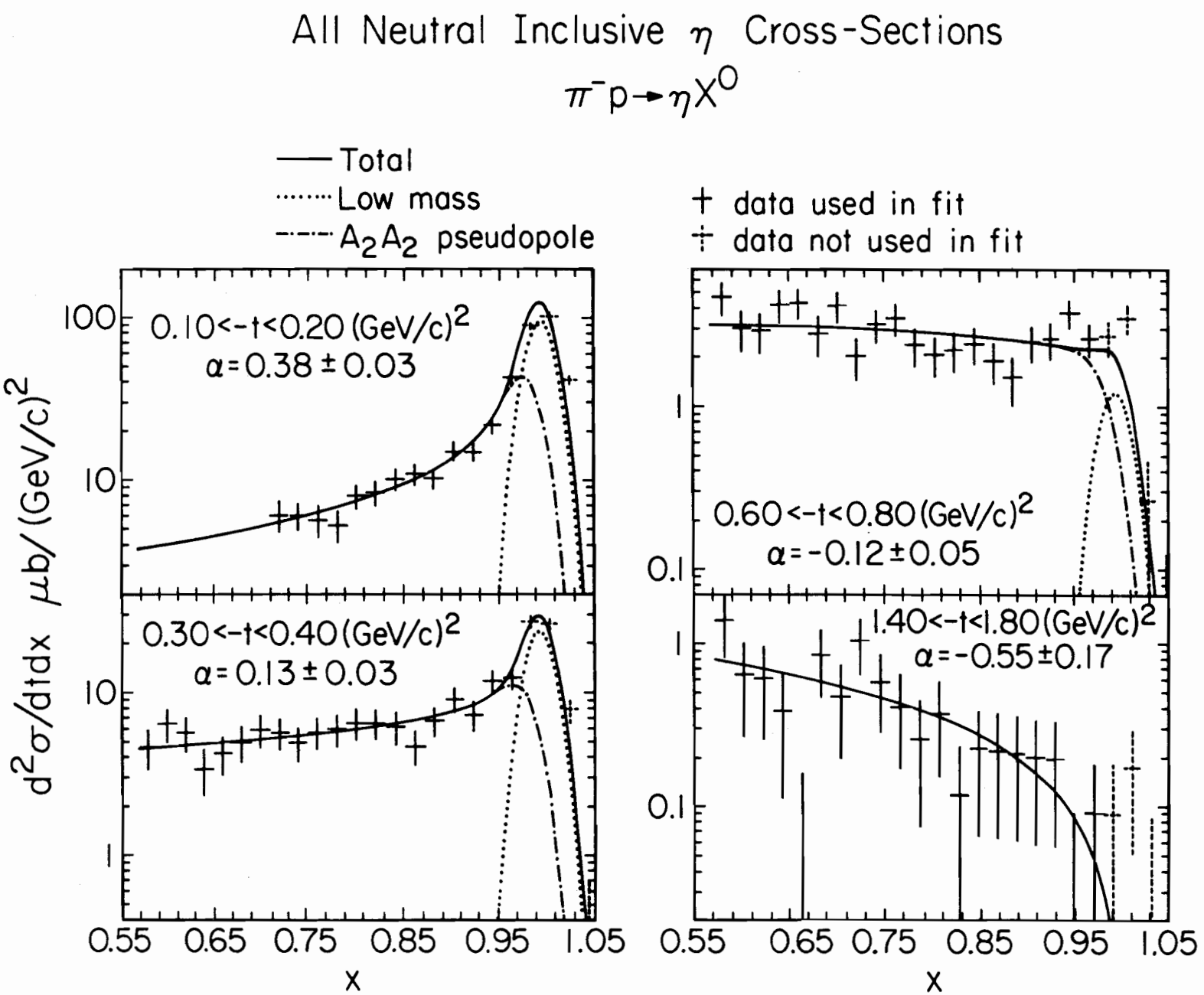
All Neutral Inclusive η Cross-Sections
π⁻p→ηX⁰
Total
Low mass
A2A2 pseudopole
data used in fit
data not used in fit
0.10<-t<0.20 (GeV/c)²
α=0.38±0.03
0.30<-t<0.40 (GeV/c)²
α=0.13±0.03
0.60<-t<0.80 (GeV/c)²
α=-0.12±0.05
1.40<-t<1.80 (GeV/c)²
α=-0.55±0.17
d²σ/dtdx μb/(GeV/c)²
x
100
10
1
0.1
0.55
0.65
0.75
0.85
0.95
1.05

Fig. 7

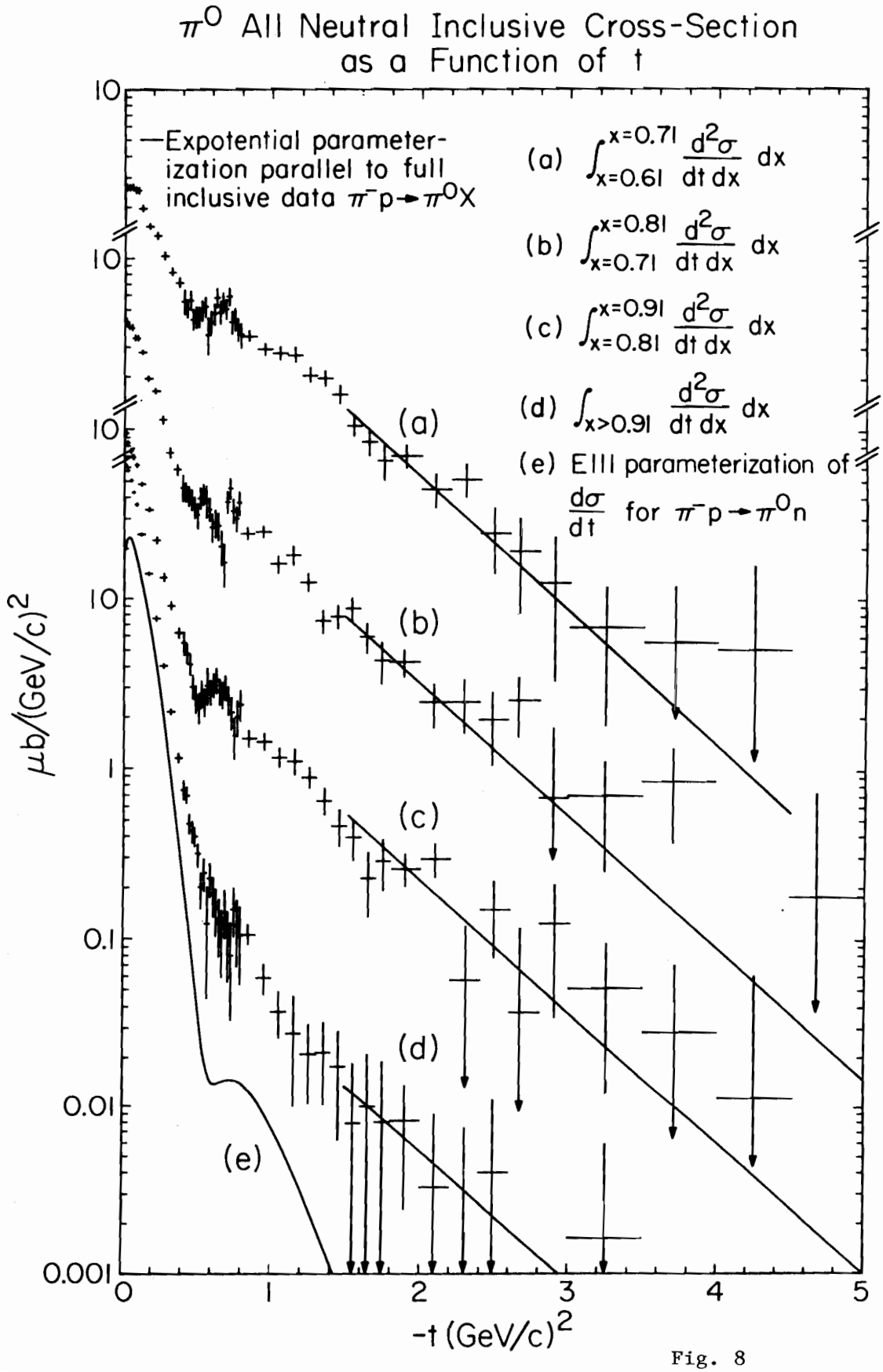
π^0 All Neutral Inclusive Cross-Section as a Function of t
—Expotential parameterization parallel to full inclusive data $\pi^- p \to \pi^0 X$
(a) $\int_{x=0.61}^{x=0.71} \frac{d^2\sigma}{dt\,dx}\,dx$
(b) $\int_{x=0.71}^{x=0.81} \frac{d^2\sigma}{dt\,dx}\,dx$
(c) $\int_{x=0.81}^{x=0.91} \frac{d^2\sigma}{dt\,dx}\,dx$
(d) $\int_{x>0.91} \frac{d^2\sigma}{dt\,dx}\,dx$
(e) EIII parameterization of $\frac{d\sigma}{dt}$ for $\pi^- p \to \pi^0 n$
(a)
(b)
(c)
(d)
(e)
$\mu b/(GeV/c)^2$
$-t\ (GeV/c)^2$
10
1
0.1
0.01
0.001
0
1
2
3
4
5

Fig. 8

Trajectories from π^0 and η All Neutral Inclusive Data

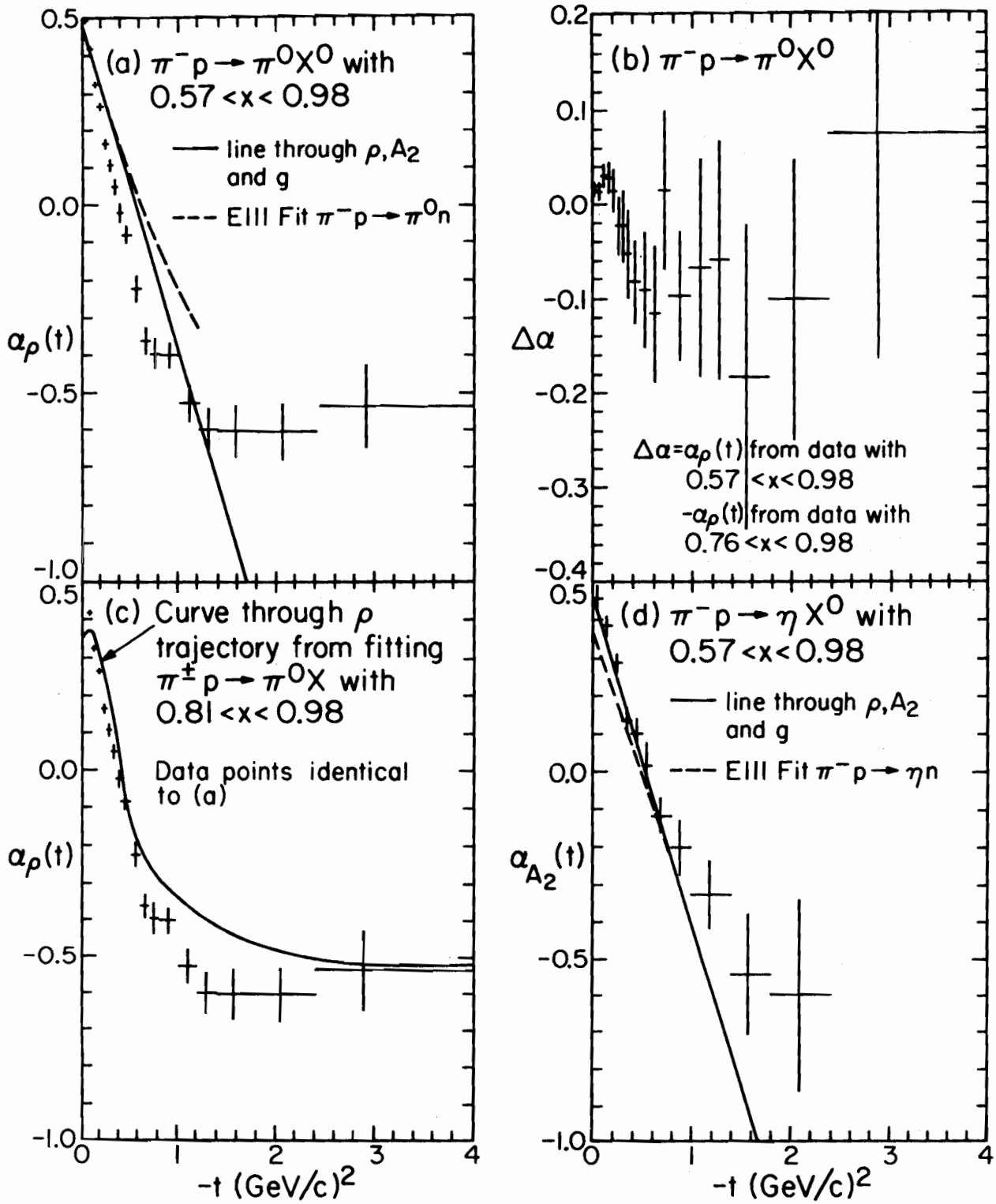

Fig. 9

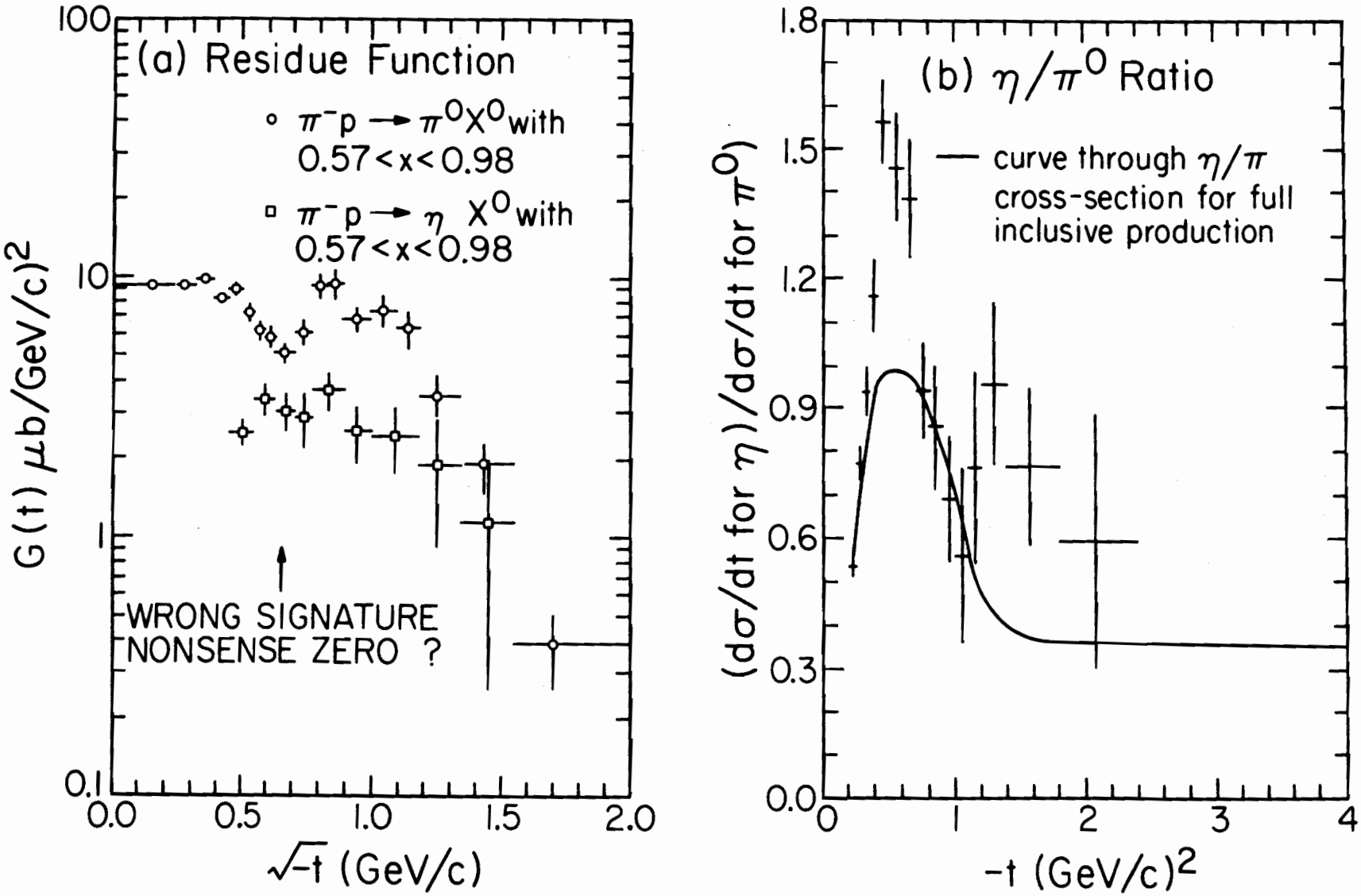
(a) Residue Function
○ $\pi^- p \rightarrow \pi^0 X^0$ with 0.57<x<0.98
□ $\pi^- p \rightarrow \eta X^0$ with 0.57<x<0.98
WRONG SIGNATURE NONSENSE ZERO ?
G(t) μb/GeV/c)²
√-t (GeV/c)
(b) η/π⁰ Ratio
— curve through η/π cross-section for full inclusive production
(dσ/dt for η)/dσ/dt for π⁰)
-t (GeV/c)²

Fig. 10